Earth and Planetary Science Letters 603 (2023) 117978

Contents lists available at ScienceDirect

Earth and Planetary Science Letters

journal homepage: www.elsevier.com/locate/epsl

Post-collisional batholiths do contribute to continental growth

Daniel Gómez-Frutos [a,b,*], Antonio Castro [a,b], Gabriel Gutiérrez-Alonso [c]

[a] Museo Nacional de Ciencias Naturales (MNCN), Consejo Superior de Investigaciones Científicas (CSIC), C. José Gutiérrez Abascal 2, 28006 Madrid, Spain
[b] Instituto Andaluz de Ciencias de la Tierra (CSIC - UGR), 18110 Granada, Spain
[c] Departamento de Geología, Universidad de Salamanca, Salamanca 37008, Spain

ARTICLE INFO

Article history:
Received 1 September 2022
Received in revised form 7 December 2022
Accepted 23 December 2022
Available online 11 January 2023
Editor: R. Hickey-Vargas

Keywords:
crustal growth
continental crust
post-collisional magmatism
metasomatized mantle
tectonics
batholith

ABSTRACT

Post-collisional voluminous silicic magmatism is represented in most orogens across the world in the form of large granodiorite batholiths and minor intermediate and mafic intrusions, postdating 5-30 Ma the age of the collisional paroxysm responsible of the main mountain building events. Post-collisional mafic intrusions are acknowledged as a mechanism that contributes to long-term yet minor continental growth. The silicic magmas forming the large batholiths, however, have been dismissed from the crustal growth discussion due to bias in the conception that they always generate by recycling older lower crustal igneous rocks. Contrary to this, geochemical and isotopic relations together with new experimental data provided in this paper suggest that the post-collisional signature can be reproduced without the implication of a crustal component, supporting a potential common origin for the two suites, intermediate and silicic. That is, both suites can be derived from a metasomatized mantle source, thus representing the injection of largely juvenile material to produce new continental crust. This inference is contextualized within the supercontinent cycle, showing that the timing of post-collisional magmatism accounts for the generation and preservation rates predicted by the existing models, since both reach maximum values in the amalgamation-collisional stage of the supercontinent cycle, rather than in the subduction stage. All together these inferences lead to think that post-Archean, post-collisional magmatism has been significantly underestimated when computing continental crustal growth through time.

1. Introduction

The existence of continental crust is one of the main differences in the evolution of the geosphere of the Earth, contrasting other planets in the Solar system. Its formation and evolution remain a fundamental discussion topic in Earth Sciences, leading to several attempts to constrain the main continental crust formation mechanisms (e.g. Arndt and Goldstein, 1987; Arndt, 2013; Condie et al., 2011; Hawkesworth et al., 2010; Rudnick, 1995). When stablishing the mechanisms by which crustal growth takes place, three requisites must be satisfied regardless of the geological setting: (1) the segregation and differentiation of igneous material from the mantle, (2) the incorporation of such material into pre-existing continental crust, and (3) its preservation in the form of large igneous bodies (Condie et al., 2011; Couzinié et al., 2016; Hawkesworth et al., 2009). Thus, since crustal growth can be fully understood by an igneous process it is safe to assert that igneous rocks constitute the best tracers to understand the processes involved in crustal growth.

The recent advance of new microanalytical techniques has allowed the development of models based on zircon isotopic composition. Particularly, Lu-Hf isotopes in zircon crystals have significantly different behaviour during partial melting in the mantle (Lu tends to concentrate in the mantle, producing higher $^{176}Hf/^{177}Hf$ ratios than those present in zircon crystals of a crustal source), and this system has been the most successful approach to discern crustal and mantle sources (e.g. Griffin et al., 2000; Kemp et al., 2006). Measurements in single zircon grains by in-situ analytical techniques (SIMS and LA-(MC)ICP-MS) have led to the elaboration of large datasets that illustrate the age when the igneous protolith separated from the mantle (Payne et al., 2016). As a result, this method has enabled the elaboration of several crustal growth models that constitute an essential contribution to the understanding of crustal growth over time (Cawood et al., 2013; Dhuime et al., 2011; Hawkesworth et al., 2010, 2019).

However, some limitations on the use of this technique have been recently pointed out. Model ages using Lu-Hf systematics suffer from similar problems to Sm-Nd system (Arndt and Goldstein,

* Corresponding author.
E-mail address: daniel.gomez@csic.es (D. Gómez-Frutos).

https://doi.org/10.1016/j.epsl.2022.117978

1987), being affected by entrainment of magmas from different sources and thus representing a hybrid age (Belousova et al., 2010; Payne et al., 2016; Roberts and Spencer, 2015). While this may be partially compensated by comparison with O isotopes, this problem is further aggravated by the reliance of these models on the number of sampled zircon grains (Hawkesworth et al., 2019; Voice et al., 2011), potentially producing fictitious density maxima, and their representativity of periods of enhanced preservation rather than crystallization (Arndt, 2013; Condie et al., 2011). Moreover, Lu-Hf systematics are unable to discriminate between largely recycled magmas from juvenile post-collisional magmatism, with the later representing the addition of new continental crust yet being invisible in the zircon record (Couzinié et al., 2016). Due to these limitations, the crustal growth estimations obtained through the use of Lu-Hf isotope systematics entail an important paradox: for being the continental crust destruction rates significantly higher in post-Archean (< 3 Ga) times due to the creation of active margins, zircon-based models predict stable low continental growth rates and low net growth (e.g. Dhuime et al., 2012, 2018; Voice et al., 2011). Furthermore, all the mentioned models rely on the equilibrium between net continental crustal growth based in crust generation in subduction related magmatic arcs and arc destruction through tectonic erosion, being the latter significantly higher in oceanic arcs than in continental arcs (Spencer et al., 2017). These models only consider collision related magmatism as a minor crustal input. That is, it is generally considered that collisional and post-collisional magmatism only recycles former igneous rocks without adding new material to the crustal budget or adding little amounts which are prone to be subsequently volumetrically compensated through lithospheric delamination and/or dripping. These observations point to a mass deficit in the continental crust that is among the most important unresolved facts in Earth Sciences.

An interesting approach to this problem that is often overlooked is the study of magmas themselves. The Earth's continents are mostly composed of igneous and meta-igneous rocks, with a bulk composition that is andesitic on average and hence classically associated with subduction (e.g. Dewey and Windley, 1981; Rudnick and Fountain, 1995). That is, continents are on average more silicic and less magnesian than basalts (SiO_2 = 65.2 wt.%; MgO = 2.5%), representing a system that is not in equilibrium with the peridotite mantle (Hacker et al., 2011; Rudnick and Fountain, 1995; Rudnick et al., 2003). The discussion about their origins has been historically focussed on the magmatic processes directly related to the subduction setting. In this regard, the most voluminous type of granite magmatism, namely I-type (Chappell and White, 2001; Pitcher, 1987), has been accountable for continental crust generation (Jagoutz and Kelemen, 2015; Rudnick and Fountain, 1995). Particularly, the subduction related I-type magmas, also named Cordilleran-type or Andean-type, are thought to be the main source of new continental crust (Barth et al., 2000; Dewey and Windley, 1981). This widely accepted statement has led to neglect the role of the more voluminous Caledonian I-type batholiths, generated in collisional orogens, especially during the post-collisional stages (Barbarin, 1999; Fowler and Henney, 1996; Pitcher, 1987), and their role in continental growth.

In this work we review the role of post-collisional magmatism as a potential continental growth mechanism using the magmas as the starting point, and not only models based in zircon crystals. We consider post-collisional batholiths as those large igneous silicic bodies emplaced substantially later (5-30 Ma) than the aftermath of the orogenic edifice building and its subsequent collapse. Analyses of published geochemical data are used to establish key differences between subduction-related (Andean-type) and post-collisional (Caledonian-type) batholiths, providing evidence that the latter have a distinct geochemical signature that departs from the subduction process. This geochemistry is put in contrast with isotopic ratios and new experimental data to unravel the controversy around the origin of post-collisional batholiths, pointing to the conclusion that crustal growth via post-collisional magmatism may have been severely underestimated. How the provided data and arguments affect the existing models or crustal growth rate estimations is out of the scope of this paper, being rather focused on the process itself.

2. The duality of I-type batholiths

The formation of I-type batholiths is known to involve crustal scale processes in two main and contrasting tectonic environments, namely subduction zones at active continental margins and post-collisional orogens in supercontinent forming orogenic belts. While the former is believed to supply enough igneous material to account for the continental growth according to volume balance (Jagoutz and Kelemen, 2015), inference based on present day outcropping magmatic rocks highlights the potential relevance of the also abundant post-collisional magmas. These are widely represented in orogenic collisional belts that have led to the amalgamation of the last four known supercontinents happening in post-Archean times, namely Nuna-Columbia, Rodinia, Pannotia and Pangea (Fig. 1).

Regarding their composition, an intriguing observation is the subtle differences between post-collisional and Andean-type magmas (Castro, 2020), even if most of these batholiths share roughly similar major oxides concentrations (SiO_2, 63–70 wt.%; FeO^T, 2–5 wt.%; MgO, 1–3 wt.%; CaO, 3–5 wt.%; Na_2O, 2–4 wt.%; and K_2O, 2–4 wt.%). This is an interesting fact considering their sources are believed to be so different, specifically partial melting of mantle-derived underplated basalts with contribution from oceanic crust in the case of Andean-type, and partial melting of old igneous lower crust with a small contribution from the mantle in the case of post-collisional type (Pitcher, 1987). Hence, it is expectable that such different settings leave a rather distinct geochemical fingerprint in the magmas.

To identify the post-collisional geochemical signature a preliminary discrimination must be made between their two characteristic suites: (1) a metaluminous (ASI<1) to slightly peraluminous silicic suite (ASI≥1.0) [ASI (Alumina Saturation Index) = molar $Al_2O_3/Na_2O+K_2O+(CaO-3.3*P_2O_5)$], mostly represented by granodiorites and the volumetrically largest of the two; and (2) a metaluminous high-K calc-alkaline suite that ranges from mafic to felsic, and is embodied by smaller intrusions (Bonin, 2004; Moyen et al., 2017). While the mafic suite has been the subject of varied studies (e.g. Couzinié et al., 2016; Fowler and Rollinson, 2012; Orejana et al., 2009), revealing particularities that will be discussed ahead, the silicic suite has historically received less attention. In this sense, we compiled a total of 2552 major element analyses that belong to the silicic suite from the most studied and well known post-collisional batholiths in the world, namely (1) the Caledonian batholiths in the northern British Isles (ca. 400 Ma), (2) the European Variscan belt, including the Iberian Massif, the French Massif Central and the Bohemian Massif (ca. 300 Ma), and (3) the Central Asian Orogenic Belt (CAOB; ca. 550-150 Ma) (Fig. 1). Compared to Andean-type rocks, post-collisional granites (*s.l.*) are always enriched in MgO and K_2O and depleted in CaO. Anomalous enrichment in MgO is mainly displayed by the most mafic terms of the series, while the high K_2O and low CaO values are widespread among the whole series. Trace elements also show an enriched signature in LILE and LREE compared to Andean-type batholiths, particularly Sr and Ba, making these rocks known as high Ba-Sr granitoids in the Caledonian belt (Fowler and Henney, 1996; Fowler and Rollinson, 2012). Nevertheless, even if trace elements provide useful information regarding the source due to its enriched nature, the systematic distinction of two magmatic se-

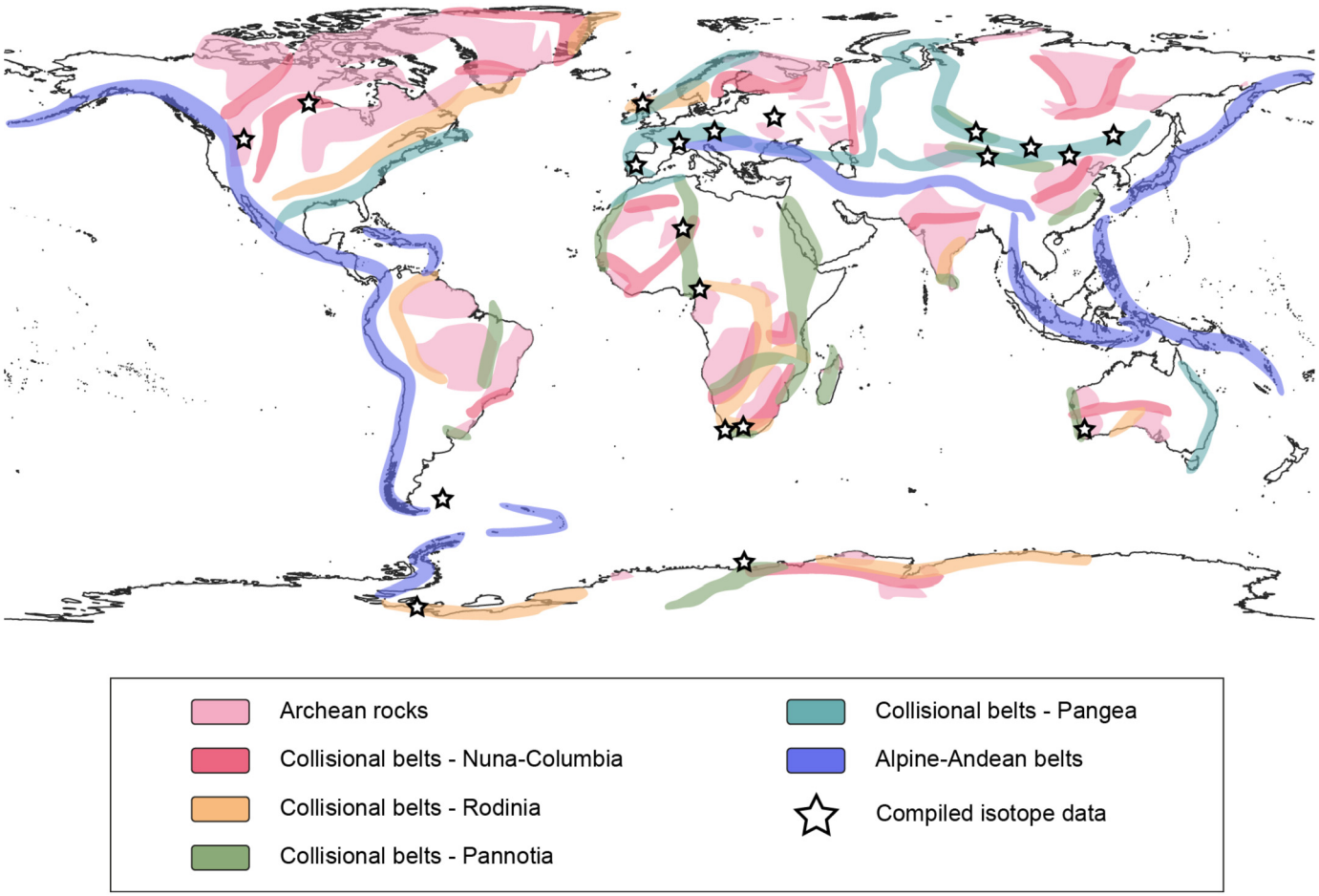

Fig. 1. Collisional belt schematic world map. Most of these collisional belts are characterized by the presence of post-collisional I-type batholiths, independently of their age. Present-day subduction related orogenic belts and recent collisional belts are also represented, in which in some cases no post-collisional batholiths are present (either they have not formed yet, or the erosion level is not deep enough yet). Compiled isotopic data locations are marked (see Fig. 3 for further details). Colour contours represent Nuna-Columbia (2.0 – 1.5 Ga), Rodinia (1.3 – 1.0 Ga); Pannotia (0.7 – 0.54 Ga); Pangea, including Caledonian, Variscan-Appalachian, Uralian and part of the Central Asian Orogenic Belt (0.4 – 0.25 Ga); and Archean. References used to the elaboration of this map can be found in the Supplementary Material 6.

ries must be established using major elements, as they record melt compositions and potential phase equilibria at the source.

The key geochemical features of post-collisional magmas may be found in Fig. 2. Samples from the characteristic Andean batholiths of Sierra Nevada and Patagonia are also plotted for comparison, showcasing the differences between the two types of I-type magmatism. The selected diagrams are the CaO–MgO plot and the Or–An–En projected space. The CaO–MgO diagram constitutes a proxy of phase equilibria since both CaO and MgO represent the most outstanding changes in liquid composition in equilibrium with a solid saturation assemblage of orthopyroxene ± clinopyroxene ± plagioclase ± amphibole, when decreasing temperature in calc-alkaline systems. This diagram shows the deviation of post-collisional batholiths, represented by Kernel density contour plots, with the three sample groups (Fig. 2a, 2b and 2c) falling underneath the plot of the Sierra Nevada and Patagonia batholiths and the Andean-type experimental cotectic line (Castro, 2021). This is due to both their depletion in CaO and enrichment in MgO. The Variscan group shows two different trends due to higher MgO values found in the French Massif Central data. Complementarily, Or–An–En diagram is a more complex representation of the system. In this diagram differences can be found in the three sample groups; Caledonian and CAOB series show density maxima towards a more intermediate composition (comparatively higher MgO), while European Variscan showcase higher K_2O concentrations. Likewise, Iberian, Bohemian and French massifs display differences, with the latter having higher MgO. Nevertheless, the most relevant aspect illustrated by this diagram is that although the composition of post-collisional batholiths is heterogeneous, there is a systematic difference respecting to Andean-type batholiths. Additional Harker diagrams can be found in Supplementary Material 1. The compiled data can be found in Supplementary Material 2.

Another key feature of post-collisional magmas is the ubiquitous occurrence of small mafic intrusions scattered around the extensive granodioritic bodies, representing the mafic end member of the high-K calc-alkaline post-collisional suite. These are usually volumetrically small compared to the large granodioritic bodies they are associated with. Due to their singular geochemistry, they have historically received several names, such as sanukitoids, vaugnerites, appinites, durbachites… (e.g. Fowler and Henney, 1996; Fowler and Rollinson, 2012; Shirey and Hanson, 1984; Smithies and Champion, 2000). This post-collisional mafic magmatism will be referred to as sanukitoids in this paper. Sanukitoids have a particular geochemical signature that sets them apart from calc-alkaline mafic magmas related with subduction settings. That is, they are enriched in MgO and K_2O and depleted in CaO compared to Andean-type magmas. Interestingly, such features are coincident with the geochemical signature displayed by the granitic terms of post-collisional batholiths. This suggests that the two suites may be related by magmatic differentiation from a common mafic magma (Fowler et al., 2001, 2008; Gómez-Frutos and Castro, 2022; Moyen et al., 2017).

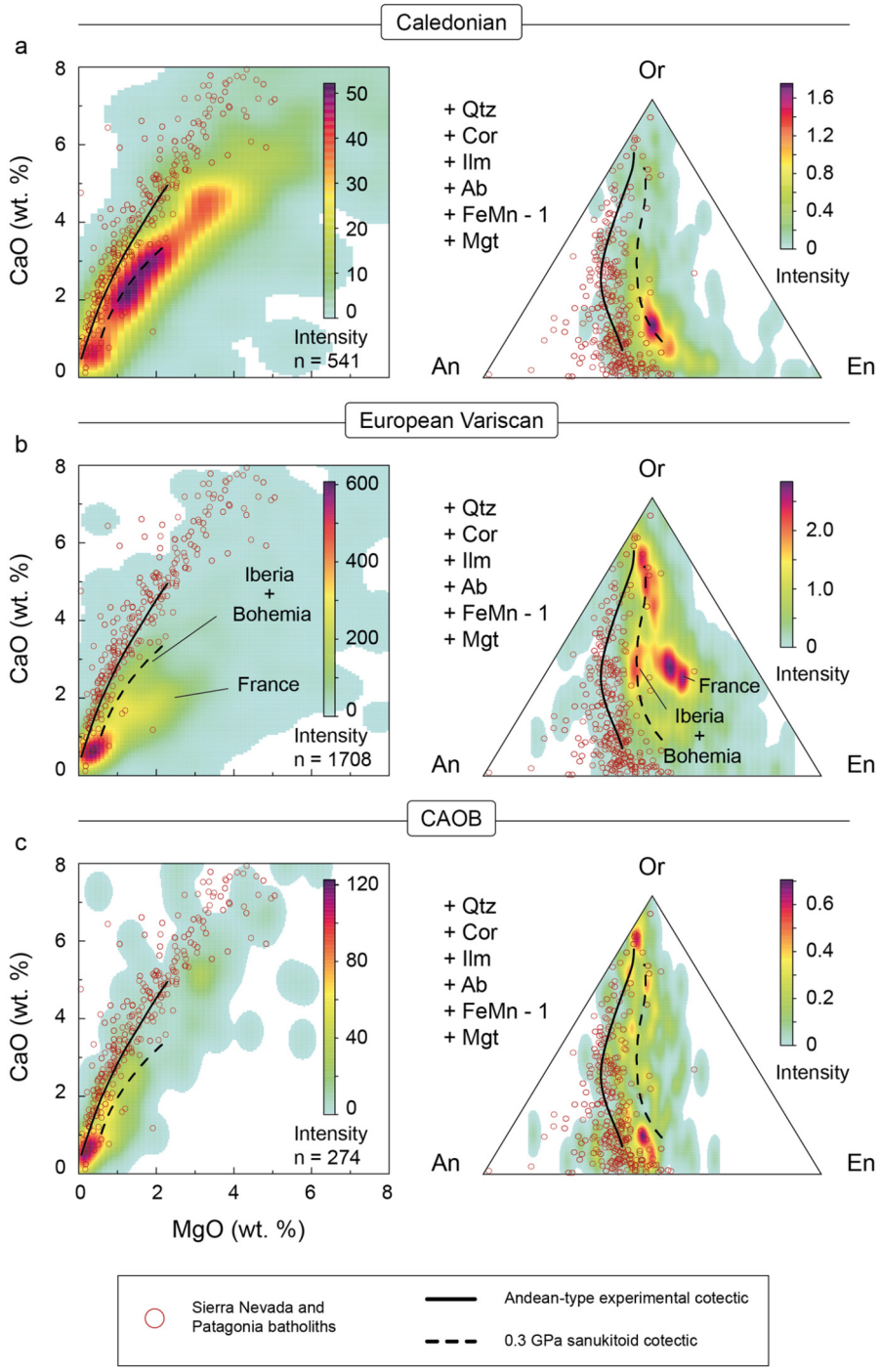

Fig. 2. Geochemical diagrams comparing three representative series of post-collisional magmatism (Kernel density contour plot) and Andean-type magmatism (red circles). (a) Caledonian series, (b) European Variscan, (c) Central Asian Orogenic Belt (CAOB). CaO–MgO diagram: post-collisional magmas are both more magnesian and less calcic than Andean-type magma. Variscan data group shows two different trends; for similar CaO values French Massif Central data are more magnesian than Iberia and Bohemia data. Or–An–En diagram: post-collisional magmas fall to the right of the Andean-type experimental cotectic array due to their Ca depletion and Mg and K enrichment. Again, by being more magnesian French Massif Central plots closer to the En pole. Andean-type data is from Sierra Nevada and Patagonia. Post-collisional magmatism and Andean-type compiled data can be found in Supplementary Material 2. Andean-type experimental cotectic line determined by Castro (2021). (For interpretation of the colours in the figure(s), the reader is referred to the web version of this article.)

The close geochemical similarity between the peraluminous silicic suite and the sanukitoids is twofold: on one hand the distinction between the two suites becomes arbitrary when exploring the geochemistry of the full series, and on the other hand, the petrogenetic relationship between the felsic and mafic endmember is conspicuous. Since the mafic endmember is widely accepted to be sourced from a metasomatized mantle source, a felsic endmember that shares most of its geochemical features must be related to that same metasomatized mantle source in some way. This observation is central to this paper.

3. The recycled isotopic signatures

The study of radiogenic isotopes systematics has provided important observations to the crustal growth discussion and granite *sensu lato* petrogenesis. Most recent studies used Hf-O systemat-

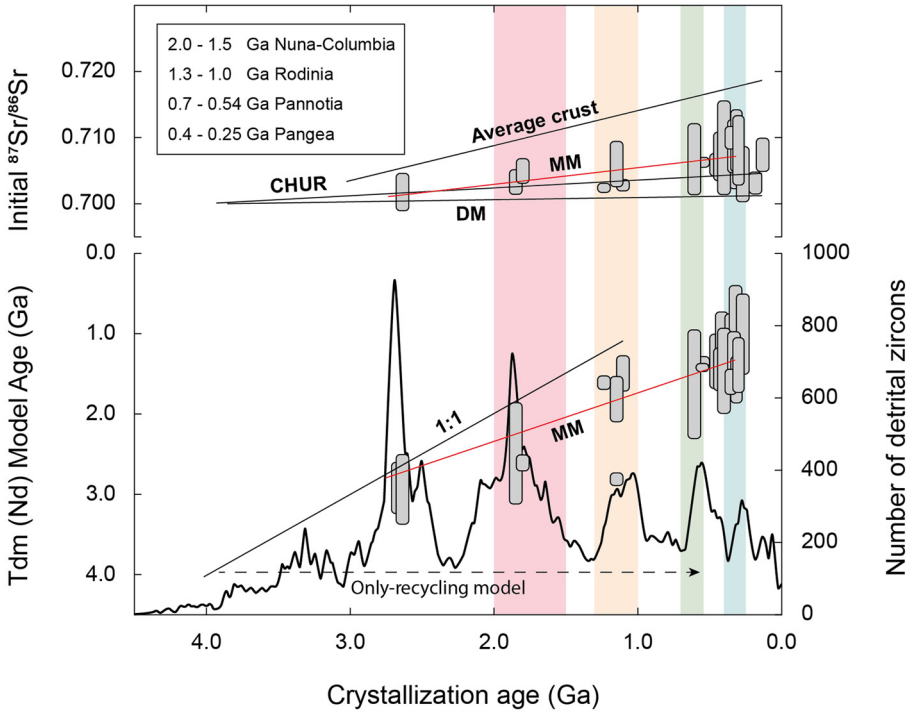

Fig. 3. Initial Sr and Nd model age against crystallization age diagrams. Detrital zircon numbers represented for comparison (Condie, 2014), providing a correlation between crustal growth predicted by number of detrital zircons and the age of the post-collisional batholiths. Initial Sr diagram shows post-collisional batholiths plot below the average crust model and towards the CHUR/DM model, suggesting a juvenile (mantle) component even when only considering granitic magmas. Model ages diagram shows that the batholiths plot following neither an only-recycling model nor an only-growth model represented by the 1:1 line. In both diagrams, the batholiths fit perfectly to the metasomatized mantle (MM) model line, pointing to a roughly similar source for both granites and mafic magmas. The MM line a linear regression of sanukitoid rocks around the world (Pearson correlation coefficient = –0.82; r^2 = 0.67). Abbreviations are as follows: CAOB, Central Asian Orogenic Belt; CHUR, Chondritic Uniform Reservoir; DM, Depleted Mantle; MM, Metasomatized Mantle. The compiled isotope data can be found in Supplementary Material 3.

ics to discuss crustal growth and estimate crustal growth rates (see references above). But even if these studies are of special use for a global approach to the problematic, the compilations are often referred to detrital zircon grains. This implies an inherent assumption that these zircon grains are sourced from weathering and transport of previously formed igneous rocks, and it is difficult to know for certain if the magmatic rocks that produced those detrital zircon grains were granitic or not. In contrast, the use of whole-rock isotopic ratios from granitic rocks is more informative about the processes of new crust generation and/or recycling, complimenting the existing Hf-O data.

When discussing post-collisional batholiths one of the most observed facts is that they always display older Sm-Nd model ages than their crystallization ages, classically interpreted to be caused by the presence of an old crust recycled component. However, it remains unclear whether the involvement of such old crust took place during mantle metasomatism, by assimilation of continental rocks during ascent or by direct batch melting of the crust to produce the magmas. In order to set this problem, we have compiled a database (768 Nd and 633 Sr analyses) of whole rock isotope data from post-collisional batholiths around the world. Pericratonic batholiths formed at the end of the Archean are also included. The compilation can be found in Supplementary Material 3.

The compiled isotope data are represented in Fig. 3. Sr initial ratios against crystallization time diagram shows that the former increase over time for post-collisional granite batholiths. These increasing ratios do not follow the 'average crustal ratio', which is otherwise followed by a fully recycled crustal material. Interestingly, most batholiths plot between the two main models, the average crust and the mantle (CHUR), implying that significant juvenile material is being supplied to generate the post-collisional magmatism, even when only granitic magmas are considered. In other words, based in the Sr isotopic signature, post-collisional granites contain a mantle (juvenile) component. On the other hand, Nd model ages plotted against crystallization time (Fig. 3) indicate that model ages (age of lithospheric residence) also increase with time. This increase has, however, a shallower slope than the depleted mantle model, implying that the model age of the batholiths is older than their age of generation. That is, a recycled (crustal and/or lithospheric mantle) component is present in the magmas. This means that part of the mass of the magmas was residing in the crust either in the form of sediments or older granitic rocks and was incorporated to the source of batholiths when they were generated at a given time, or that they represent melting of the subcontinental lithospheric mantle. These observations limit the viability of two models: (1) if granites formed following an 'only-recycling model' that affects a primitive (Archean) granitic crust, they must follow a flat time evolution with a constant model age through time. (2) If, by contrast, granite magmatism represents a net addition of magma to the crust from a depleted sublithospheric mantle, the batholiths will plot on the 1:1 line, representing an 'only-growth model', since model ages and crystallization ages should be identical. None of these models are satisfied due to the mixed signature displayed by the Sm-Nd data from post-collisional batholiths.

Nevertheless, a third possibility is that the magmas originate in a metasomatized mantle source. By being sourced in an enriched mantle, the batholiths will plot along an intermediate line. A model line of metasomatized mantle post-collisional magmatism is plotted for comparison. This line is a linear regression of sanukitoid data (rocks with mafic-intermediate compositions, SiO_2 < 63 wt.%) from several different batholiths (Supplementary Material 3). Interestingly, the model line overlaps the trend of the studied batholiths. This observation tallies with the common ma-

jor element signature displayed by post-collisional granites (*s.l.*) and associated sanukitoids, and it can only be explained if the two types of magmas originate in closely similar processes. This is of special interest when considering the controversial origin of the post-collisional magmatism.

4. Origin of post-collisional batholiths

Holding post-collisional magmatism responsible for the generation of new continental crust implies a deep understanding of the origin of such magmas, since crustal growth entails the entrainment of juvenile mantle material to the continental crust. While some existing models do propose a mantle origin for post-collisional batholiths (Fowler and Henney, 1996; Fowler et al., 2001; Hildebrand and Whalen, 2017), several other models to explain the origin of these magmas are based on the initial premise that significant volumes of magma are produced by lower crust melting (e.g. Annen et al., 2006; Aranovich et al., 2014; Petford and Gallagher, 2001). However, there are significant variables that are commonly dismissed in the continental crust melting models:

(1) The lower crust is mafic on average (Rudnick and Fountain, 1995). A hypothetical basalt precursor in the lower crust for the batholiths entails the need for the elimination of an ultramafic residue from the lower crust in order to produce the observed bulk composition. In contrast, implication of an already fractionated andesitic precursor will provide the needed composition to form the continental crust skipping the problem of a missing ultramafic residue.
(2) The lower crust is essentially depleted. Simple melting of the lower crust cannot reproduce the enriched signature of post-collisional batholiths. An additional element in the process needs to be involved.
(3) The crust showcases unrealistically high solidus temperatures (>850°C) that are incapable of producing significant amounts of liquids even when periodic influx of mafic magma is invoked (Bonin, 2004). Thus, water is a necessary addition to lower the solidus even more (e.g. Aranovich et al., 2014; Castro, 2020; Collins et al., 2016; Weinberg and Hasalová, 2015).
(4) However, this consideration entails yet another problem, since even with the most conservative estimation of 4 wt.% H_2O dissolved in the parental magma (Plank et al., 2013) the water content in a residual granitic liquid that represents a 0.2 melt fraction will have ~20 wt.% H_2O. This water amount in residual liquid is unrealistic and is not supported neither by the observed igneous textures in the rocks nor by the scarcity of pegmatitic dykes in the plutons.
(5) Fully recycled lower crust inherently implies a recycled isotopic signature. Nevertheless, as shown in the previous epigraph the rocks show an important mantle component in their Sr and Nd isotopes.

While these issues represent an ongoing debate, they have highlighted the importance of sanukitoid as heat and water donors for water-fluxed melting. Additionally, they are also capable of resupplying incompatible elements to the lower crust, particularly K_2O, Sr and Ba (Smithies et al., 2021). In summary, all the aforementioned arguments are consistent with a petrogenetic relationship between metasomatized mantle magma and post-collisional granites. Accidental phenomena such as magma mixing and/or crustal assimilation cannot account for the world-wide uniform geochemistry, the cotectic patterns followed by the rock series and the trends displayed by their isotopic signatures.

Taking sanukitoid rocks into account, previous experiments have attempted to constrain their role in the process. Results provide key insights on the topic, such as the importance of a dominant harzburgitic source (Wood and Turner, 2009), and the inability to reproduce the post-collisional signature by melting of a mixed sanukitoid and granulitic compound representative of the lower crust (Castro, 2020) or by sheer differentiation (Gómez-Frutos and Castro, 2022), with the latest work providing evidence that differentiation at shallow depth do reproduce the post-collisional geochemical signature, and that lower crustal pressures (c.a. >1.0 GPa) produces Ca-depleted melts. With this background and following the common conception that the crust is involved in the process, we performed a new set of experiments to test the importance of varying sanukitoid-crust proportions and its impact on the liquid composition. Selected pressures were 1.0 GPa and 0.5 GPa to simulate differentiation at the crust-lithospheric mantle boundary and at emplacement level.

Table 1
Composition of the starting materials.

	Starting materials		Model compositions		
	A208-22	5Q-92	Middle crust average[1]	Pilbara Suite[2]	Superior Province[3]
SiO_2	70.22	60.36	69.4	61.86	58.95
TiO_2	0.44	0.88	0.33	0.51	0.54
Al_2O_3	15.15	15.59	16.21	14.48	17.79
FeOt	3.11	6.03	2.72	5.64	5.22
MgO	1.00	4.30	1.27	4.17	4.58
MnO	0.07	0.13	0.03	0.08	0.10
CaO	3.17	5.34	2.96	4.67	4.94
Na_2O	3.42	3.97	3.55	3.91	4.21
K_2O	2.39	2.18	3.36	1.8	3.1
P_2O_5	0.13	0.52	0.15	0.24	0.30
LOI	0.91	0.7	-	2	-
Total	100	100	99.98	97.36	99.73

Composition recalculated to an anhydrous base. Total iron as FeO.
[1] Middle crust average; Rudnick et al. (2003).
[2] Pilbara suite sanukitoid; Smithies and Champion (2000).
[3] Roaring River Valley Complex sanukitoid. Canadian Superior Province; Stern et al. (1989).

4.1. Experimental approach

The process was tested using representative compositions for both components (Table 1), namely a mafic enclave (5Q-92) from Los Pedroches batholith in the Variscan complex Iberian Massif in SW Iberia as the sanukitoid component, and a granodiorite (A208-22) from the Andes volcanic arc that also resembles the average composition of the middle crust (Rudnick et al., 2003). 5Q-92 mafic enclave was already used in former experimental work and is already justified to be representative of the common nature of sanukitoids after comparing it with the sanukitoid world series (Gómez-Frutos and Castro, 2022). A208-22 granodiorite exhaustive description can be found in previous works (Castro et al., 2011).

Prior to the interaction experiments the mafic enclave was hydrated with 3 wt.% H_2O and melted at 1200°C to produce a natural glass and minimize the existence of relict crystals. The resulting hydrated glass was grounded to a fine powder and mixed with the A208-22 granodiorite into different proportions 1:1, 1:3, 3:1. The mixtures were milled and homogenized to enhance the process by simulating grain-to-grain interactions, and then used for six experimental runs. Additionally, four more runs were performed only with the granodiorite, two of them with an additional 3 wt.% H_2O (experiments are labelled as w, standing for water-bearing; and nw, standing for no water in Table 2). Sanukitoid-only experiments were also performed, in this case with a varying range of temperature due to the system being mafic-intermediate and thus having higher liquidus temperatures. Granodiorite and mixtures runs were carried to temperatures of 1000°C and pressures of 1.0 GPa and 0.5 GPa. Correspondingly, the three runs using only sanukitoid were carried to 1000, 1050 and 1100°C and 1.0 GPa.

Table 2
Experimental glasses.

Run	Duration (hours)	Mix (A208-22:5Q-92)	T (°C)	P (GPa)	*n*	SiO_2	TiO_2	Al_2O_3	FeO^T	MgO	MnO	CaO	Na_2O	K_2O	P_2O_5	*F*	Total
D21-19	50	1:3	1000	1.0	14	65.41	0.57	14.90	2.47	0.95	0.07	2.57	2.82	2.94	0.32	0.28	93.13
						1.42	*0.05*	*0.40*	*0.22*	*0.19*	*0.02*	*0.31*	*0.27*	*0.30*	*0.11*	*0.12*	*0.60*
D21-19	50	1:1	1000	1.0	13	67.82	0.46	13.63	2.01	0.72	0.07	1.98	2.83	3.30	0.29	0.18	93.14
						0.97	*0.06*	*0.61*	*0.11*	*0.22*	*0.02*	*0.46*	*0.28*	*0.19*	*0.13*	*0.12*	*0.53*
D21-19	50	3:1	1000	1.0	14	69.20	0.42	13.09	1.70	0.47	0.05	1.41	2.78	3.57	0.19	0.13	92.90
						0.75	*0.10*	*0.31*	*0.07*	*0.03*	*0.02*	*0.05*	*0.19*	*0.15*	*0.12*	*0.07*	*0.84*
D21-20	95	1:3	1000	0.5	5	66.12	0.65	15.05	2.45	1.29	0.09	2.90	2.69	2.71	0.44	0.20	94.41
						0.46	*0.07*	*0.40*	*0.09*	*0.04*	*0.02*	*0.06*	*0.47*	*0.30*	*0.09*	*0.02*	*0.39*
D21-20	95	1:1	1000	0.5	11	70.11	0.55	13.94	2.10	0.70	0.05	1.87	3.05	3.47	0.28	0.10	96.09
						0.66	*0.05*	*0.31*	*0.15*	*0.05*	*0.02*	*0.09*	*0.22*	*0.09*	*0.14*	*0.03*	*0.64*
D21-20	95	3:1	1000	0.5	3	72.96	0.80	12.75	2.11	0.38	0.03	0.59	2.72	3.75	0.29	0.07	96.30
						1.11	*0.03*	*0.55*	*0.05*	*0.04*	*0.01*	*0.06*	*0.35*	*0.55*	*0.14*	*0.02*	*0.64*
D21-23w	69	1:0	1000	1.0	5	66.55	0.33	14.35	1.58	1.03	0.07	2.35	3.19	2.19	0.06	0.14	91.78
						0.97	*0.03*	*0.45*	*0.11*	*0.09*	*0.03*	*0.14*	*0.41*	*0.05*	*0.02*	*0.03*	*0.69*
D21-23nw	69	1:0	1000	1.0	5	69.13	0.37	13.10	1.28	0.42	0.05	0.91	2.72	4.00	0.18	0.08	92.15
						0.38	*0.02*	*0.23*	*0.06*	*0.02*	*0.01*	*0.02*	*0.12*	*0.05*	*0.12*	*0.04*	*0.63*
D21-24w	50	1:0	1000	0.5	6	66.05	0.41	14.82	1.89	1.08	0.06	2.44	3.41	2.23	0.12	0.12	92.55
						1.40	*0.05*	*0.77*	*0.25*	*0.19*	*0.01*	*0.34*	*0.07*	*0.08*	*0.06*	*0.04*	*0.46*
D21-24nw	50	1:0	1000	0.5	5	69.82	0.38	12.96	1.43	0.43	0.05	0.88	3.40	3.90	0.13	0.08	93.40
						0.71	*0.08*	*0.33*	*0.17*	*0.06*	*0.02*	*0.14*	*0.04*	*0.08*	*0.05*	*0.02*	*0.53*
D22-1	70	0:1	1000	1.0	21	66.71	0.58	15.16	2.31	0.72	0.06	1.77	3.15	4.6	0.14	0.29	95.22
						1.06	*0.08*	*0.41*	*0.16*	*0.10*	*0.02*	*0.20*	*0.33*	*0.35*	*0.02*	*0.03*	*0.69*
D22-2	50	0:1	1050	1.0	7	65.03	0.80	16.33	3.77	0.94	0.09	2.37	3.17	3.40	0.23	0.27	96.13
						0.66	*0.08*	*0.53*	*0.24*	*0.16*	*0.03*	*0.18*	*0.22*	*0.34*	*0.04*	*0.02*	*0.71*
D22-10	44	0:1	1100	1.0	11	59.66	1.25	17.07	3.43	2.23	0.10	4.18	3.90	3.19	0.63	0.17	95.65
						1.43	*0.17*	*0.55*	*0.34*	*0.43*	*0.02*	*0.56*	*0.25*	*0.16*	*0.15*	*0.02*	*0.70*

n, number of analyses. Numbers in italics below each wt.% are standard deviations.

A total of thirteen experimental runs were performed. Run durations exceeded two days in most cases and are reported in Table 2. Results will allow to compare liquid compositions in four case scenarios: (1) heat triggered melting of the granodiorite, (2) fluid-fluxed melting when water is added directly into the granodiorite, (3) fluid-fluxed melting when water is supplied by a mafic magma, and (4) sanukitoid only melting. A detailed description of the experimental and analytical techniques can be found in Supplementary Material 4.

4.2. Experimental results

Synthesized products consist of homogeneous glass and mineral assemblages. Glass major element measurements display standard deviations lower than unity. Solid phases are mostly constituted by variable proportions of orthopyroxene, clinopyroxene, amphibole, plagioclase and quartz as the main phases, and magnetite and apatite as common accessory phases. Relict crystal prevention with the formerly described method was mostly successful, with the exception of traces of relict albite-rich plagioclase cores that may be found in the assemblages. Modal proportion calculations performed with MINSQ spreadsheet (Herrmann and Berry, 2002) result in residual values lower than two. Additionally, glass modal proportion and Mg# [=molar MgO/(MgO+FeO^T)] increases with increasing the fraction of 5Q-92 in the mixtures (Fig. 4). All these considerations together suggest that equilibrium was successfully attained. It is also worth noting that sanukitoid only run at 1050°C (D22-2) display anomalously high FeO contents in the synthesized glass in comparison with the 1000°C and 1100°C runs (D22-1 and D22-10, respectively).

Glass measurements for all experimental runs with their respective standard deviations are displayed in Table 2. Major element and glass modal abundance are plotted in comparison with post-collisional granodiorites ($63 < SiO_2 < 70$; Fig. 4). The silica interval is restricted after the natural observation that granodiorites embody the largest volumes of intrusive rocks within post-collisional batholiths. The plotted experimental glasses suggest that increasing Andean-type component (A208-22) deviates the composition from the observed natural trend, the only exception being K_2O. The synthesized glasses are also plotted in the two selected classification diagrams and additional Harker diagrams (Fig. 5). Regardless of the mix proportions all synthesized glasses using A208-22 (crustal component) fall within the error intervals of the Andean experimental cotectic line (Castro, 2021), and on top of the Andean-type calc-alkaline array. Increasing proportions in the mafic component when the crustal component is present only pushes the resulting liquid into a more mafic yet typical Andean-type composition. Granodiorite-only runs also fall in the same area, with the water-bearing runs being constituted mainly by liquid and thus falling near the starting material composition. Comparatively, runs using only sanukitoid successfully reproduce the post-collisional geochemical signature, being depleted in CaO, enriched in K_2O and within the expected MgO density range for their respective silica values. Phase analyses and modal proportions can be found in Supplementary Material 5.

5. Discussion

5.1. Continental crust melting

The classical works on I-type magmatism defined the origin of post-collisional magmas as 'infracrustal', or 'below the crust' (Chappell and Stephens, 1988). Contrarily to this genetical definition, several works containing the term 'infracrustal' have attempted to unravel the crustal source of post-collisional batholiths (e.g. Bonin, 2004; Pitcher, 1987). This is paradoxical considering the several problems entailed by lower crust melting models (see above). And more importantly, they are contrary to the insights provided by the experimental results.

First, the most important implication of our experimental results is that the post-collisional geochemical signature can be reproduced by using only sanukitoid (metasomatized mantle) starting material (Fig. 5). Contrarily, experimental runs using a crustal component depart from the post-collisional signature, suggesting that the geochemical features of the melts are fully controlled by the Andean liquid line of descent rather than by the varying proportion of mafic mantle magma supplied to the crust. In other words, melting of an Andean-type granodioritic source and further contamination with a mafic end-member push the magma towards

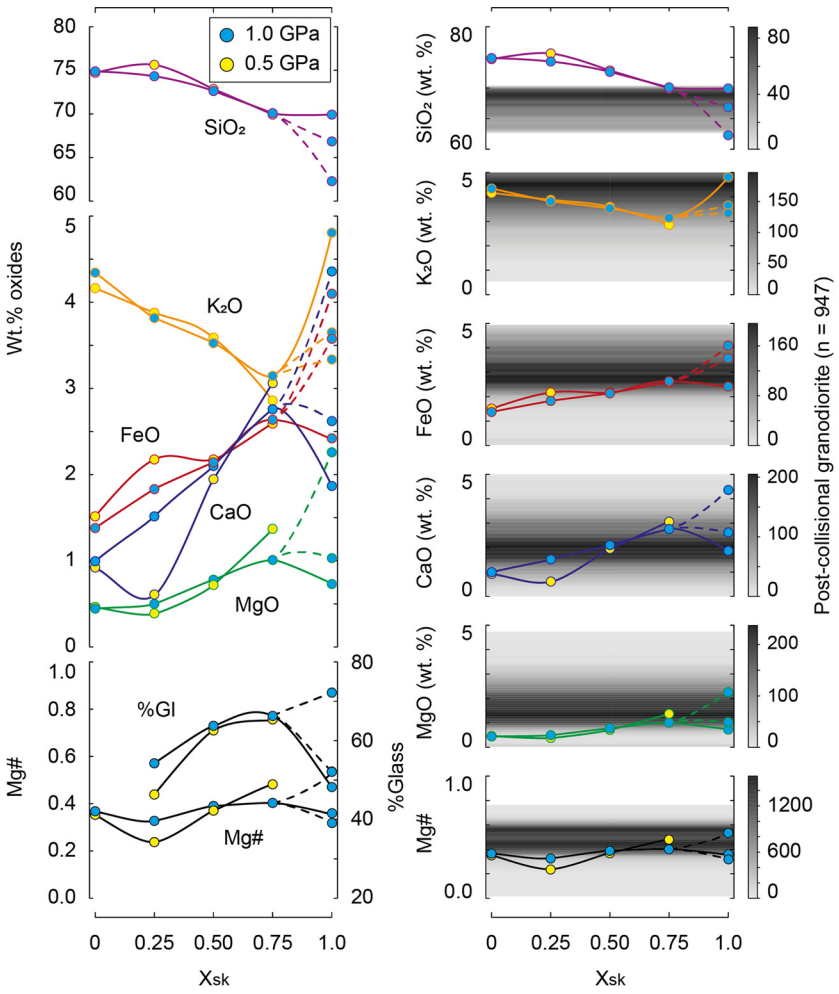

Fig. 4. Sanukitoid (sk = 5Q-92) mixture proportion against major element concentrations in experimental glass and modal glass fraction. Each circle represents an experimental run. Experimental glasses using 100% sanukitoid at 1000°C, 1050°C and 1100°C show coherent major element patters, increasing MgO and CaO and decreasing K_2O and SiO_2 when increasing temperature. Run at 1050°C show anomalously high FeO content and low Mg#. Kernel density plots post-collisional granodiorites ($63 < SiO_2 < 70$) for comparison. Restricted silica interval is selected after natural inference of the most voluminous bodies found in post-collisional batholiths being granodioritic. Major elements of experimental glass suggest that increasing the Andean-type component (A208-22) deviates the composition from the observed natural trend, the only exception being K_2O. Both glass proportion and Mg# increase with increasing sanukitoid component in the mix runs (and thus the H_2O content). Sanukitoid only runs show a decrease in glass proportion, coherent with a fully intermediate-mafic system having higher liquidus temperatures. Pressure does not seem to have a significant effect on neither of the parameters represented.

more mafic compositions (black circles, Fig. 5), but does not reproduce the low Ca and high Mg and K contents of post-collisional batholiths. Previous experimental studies performed with granulitic starting materials resembling a mafic lower crust have not successfully reproduced the post-collisional geochemical signature either (Castro, 2020).

The inherent implication of these observations is that the major element geochemistry of post-collisional batholiths is satisfied only when the crust is excluded from the process, thus granitic (*s.l.*) magmas representing fractionates from an intermediate magma that generated in a metasomatized mantle source (Fig. 6). This conclusion eliminates several problems entailed by the lower crust melting model. By coming from the mantle, temperature and water are no longer a limitation when considering the high solidus of this system. Moreover, the solid residue of the sanukitoid system is mainly constituted of plagioclase and pyroxene, and thus is compatible with the noritic composition of the lower continental crust (Meissner et al., 1986).

Besides, the hypothesis that a trachiandesitic (sanukitoid) magma from a metasomatized mantle source is the precursor of the granitic batholiths is also supported by the isotopic arguments provided in this paper (Fig. 3). Whole-rock isotopes show not only that the batholiths do not follow an only-crustal array, but also the exact overlap between isotopes from sanukitoid and granitic rocks, the former represented by the metasomatized-mantle (MM) model line. The fact that evolved isotopic signatures are present in the more mafic terms of the series makes crustal processes of contamination and magma mixing unlikely, since no correlation is observed with characteristic crustal contaminants such as Si and K. Hence, the only plausible explanation that satisfies all observations is that the recycled signature was already present in a mantle source.

Nevertheless, even if all collected evidence points to a mantle source for the post-collisional magmatism, some drawbacks of the model must be addressed. Previous experimental results using sanukitoid-only starting material (5Q-92) at 0.3 GPa provide interesting insights on the problem. While the geochemical signature is indeed reproduced by 0.3 GPa differentiation of a sanukitoid parental magma (0.3 GPa sanukitoid experimental cotectic, Fig. 5), shallow depth differentiation for the mantle magmas implies the generation of a solid residue that is absent in the batholiths at the level of final emplacement and crystallization. On the other hand, 1.0 GPa differentiation eliminates the problem of the shallow residue, since it stays in the lower crust and accounts for its gran-

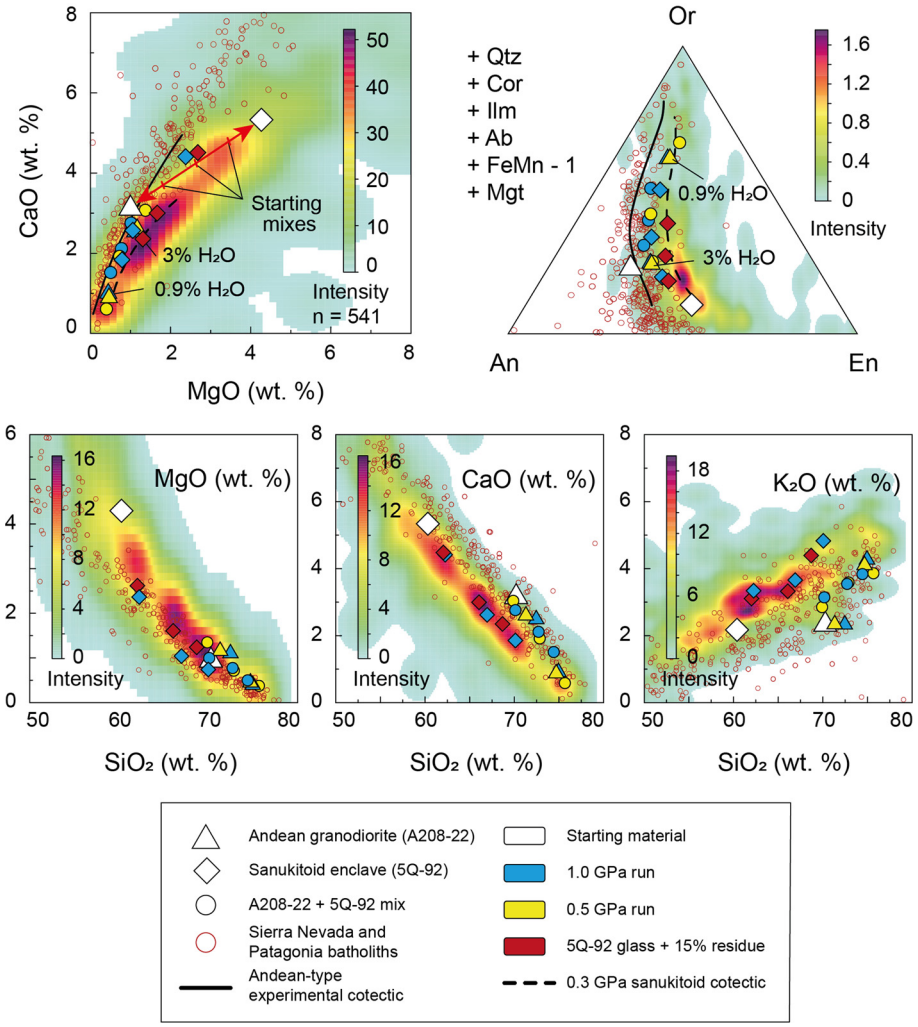

Fig. 5. Selected diagrams and additional Harker diagrams with the experimental liquids plotted. For the runs using mixes higher CaO and MgO equals to higher mafic component in the mix. The Kernel density plot represents the British Caledonian batholith. The experimental liquids from mixes follow the Andean-type cotectic array, showing no deviation towards post-collisional signature when increasing the mafic component. Liquids from using only Andean granodiorite (A208-22) also have Andean-type geochemistry, regardless of the water content. Sanukitoid (5Q-92) only runs have post-collisional geochemical signature, following the post-collisional density maxima in CaO and K_2O Harker diagrams. Mixing of sanukitoid liquids with 15% of the experimental solid residue improves the MgO values, resulting in a composition that fully matches the post-collisional geochemical signature.

ulitic nature (Fig. 6), but slightly higher MgO values are observed in the rocks than in the synthesized products (blue squares, Fig. 5). Further explanations must be provided to account for this ambiguity. In this regard, we find of special interest the widespread presence of amphibole aggregates (clots) that represent relic pyroxene crystals (Stephens, 2001), together with relic plagioclase cores, in many post-collisional plutons. These observations point to the conclusion that the rocks represent a system that was not 100% liquid, with the magmas most likely dragging suspended solid material either from the source or from a putative magma chamber. Experimental results suggest that the incorporation of crustal material (granite) pushes the composition towards Andean-type affinity, thus excluding the interaction with a crustal contaminant as the cause of post-collisional magmatism. Moreover, to account for a ubiquitous feature of magmas, namely the off-Andean post-collisional array (Fig. 2), the incorporated material must be available regardless of the specific setting. This is only explained if the contaminant is an intrinsic characteristic of the system and not an accidental contaminant. We propose that mafic contaminants are represented by minerals as pyroxene or amphibole entrained within the magmas as either early crystalized cumulates or restitic phases from a mantle ultramafic source (Fig. 6). To test this hypothesis, the sanukitoid experimental liquids were mixed with 15% of the experimental residue. This value is calculated after checking different mix proportions and testing which one satisfies the post-collisional geochemistry best. Interestingly, the resulting composition falls in the post-collisional array (red squares, Fig. 5). This estimation is also supported by the relatively common reaction textures that are observed on the rocks. Specifically, relict cores of anortite-rich plagioclase are common in granodiorites and enclaves. Also, amphibole clots are widely present in the rocks of the series. This can be explained by shallow depth re-equilibration of the liquids, as shown by the 0.3 GPa sanukitoid experimental cotectic (Gómez-Frutos and Castro, 2022). Furthermore, a geochemical signature partially caused by a variable self-contamination process that behaves like an open system is coherent with the heterogeneity displayed by post-collisional rocks. While this contamination mechanism can also occur in the Andean-type system, the scarcity of orthopyroxene causes the whole composition of the residue to be colinear with the cotectic. Thus, the contaminated liquids are displaced along mixing lines close to the cotectic line (Castro, 2021, his Fig. 3). Furthermore, a high residence time in the crust while slowly cooling is expected to re-equilibrate the mag-

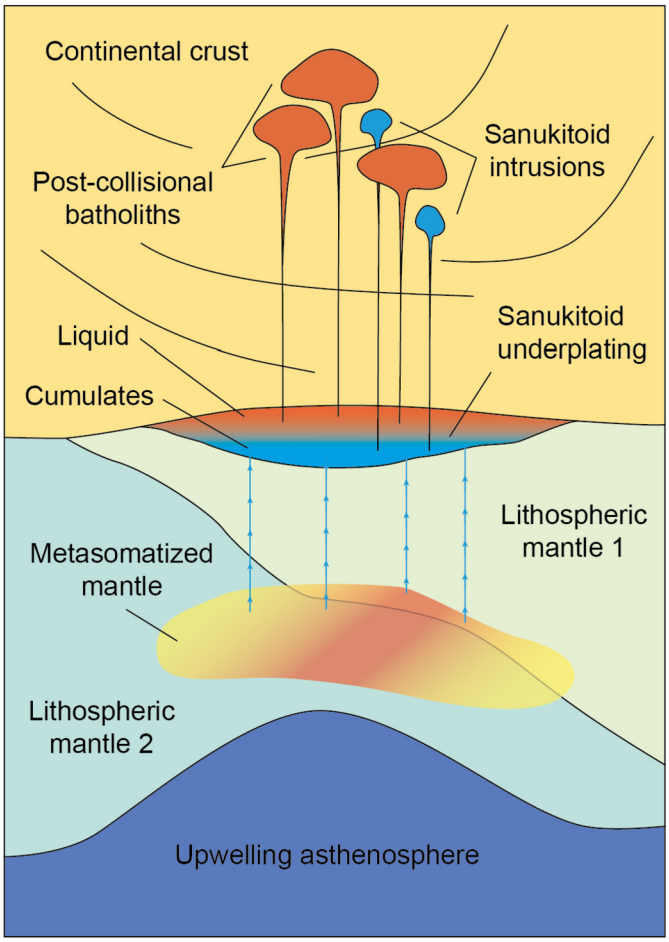

Fig. 6. Schematic petrogenetic model for post-collisional magmatism. Asthenosphere upwelling heats the pre-existing metasomatized mantle, potentially triggering melting. Subsequent sanukitoid melts ascend and underplate in the high rheology contrast surface between the crust and the lithospheric mantle. Due to density contrast differentiated liquids rise and cumulates sink. Extracted melts drag cumulate phases due to their high availability, resulting in the heterogeneous geochemistry displayed by post-collisional batholiths. After all melt extraction has occurred leftover cumulate material joins the lower crust, accounting for its depleted nature. This whole process represents the addition of a considerable amount of igneous material to the continental crust from the underlying metasomatized mantle.

mas into the low-Ca and high-Mg observed signature, erasing any former evidence of disequilibrium.

In summary, our experimental results support an origin of post-collisional batholiths in which the continental crust is not involved directly in the process. This consideration, together with the isotopic and physical evidence, points to the conclusion that the post-collisional granites share a common source with the mafic magmas they appear associated with. That is, they both come from a metasomatized mantle source.

On a final note, the origin of this metasomatized mantle and geodynamic processes leading to mantle melting and post-collisional magma generation are a topic that need of further discussion. It has been argued in arc related environments that melts and/or fluids from a subducted slab are unable to transport the trace element budget that characterize intermediate magmatism, being necessary the whole material present in subducted mélanges of oceanic crust sediments (Castro et al., 2013; Nielsen and Marschall, 2017). This metasomatism may be the result of multiple subduction events, and not only the most recent one, as shown by the wide range of model ages in post-collisional magmas (Fig. 3). Moreover, the preferred mechanism to trigger melting is a combination of decompression and heating due to mantle upwelling (Fig. 6). This is a plausible scenario according to thermomechanical models in collisional orogens (e.g. Faccenda et al., 2008; Ueda et al., 2012). Although post-collisional magmatism differs from arc magmatism (see above), the interaction between mantle and subducted materials is needed in both cases. However, note that these considerations are merely speculative and depicting an accurate model is beyond the scope of this paper. Hence, this topic should and will be the subject of future works, most preferably combining the information given by new experiments and thermomechanical models.

5.2. Implications for crustal growth

Data provided in the former epigraphs aimed to unravel the origin of the batholiths, pointing to the conclusion that they were originated in the mantle. This premise has direct consequences in the crustal growth discussion in several different aspects. Evidence of granodioritic magmas sourced in the mantle represents a major issue when addressing the origin of continents, since the post-Archean continental crust is estimated to be constituted by andesites or granitoids of granodioritic affinity (Hacker et al., 2011; Rudnick et al., 2003). Crustal growth for a given time interval is calculated by the volume of continental crust generated from the mantle minus the amount immersed and assimilated back into the mantle (Condie and Aster, 2010). In other words, two main points must be addressed when discussing crustal growth over a given process, namely generation of the magmas and preservation rates. In this regard, the timing of the magmatic process is of special relevance, since it has a direct impact on both aforementioned factors.

Work on zircon large datasets has recently been the focus of crustal growth studies, allowing for a global view of the supercontinent cycle and crustal growth intervals (Dhuime et al., 2018). While Hf-O systematics have limitations, specifically when used on detrital zircon grains for petrogenetic purposes, they trace the occurrence of big magmatic events and their timing within the supercontinent cycle. If post-collisional magmatism produces new continental crust, the assembly of supercontinents and their related orogenic process must be correlated with maxima in the continental crust production. In this regard, accretionary orogens have been active continuously throughout a major part of the Earth history and constitute major sites of continental growth (Cawood et al., 2006). Accordingly, the peak of crustal growth for each supercontinent cycle is coincident with the post-collisional stage (Condie and Aster, 2010; Hawkesworth et al., 2010; Hildebrand and Whalen, 2017). This observation makes no sense other than the batholiths representing juvenile injections to the continental crust.

Equally important, preservation is widely known to be a key factor when considering the net growth of the continental crust. Not only that, but recent work has also even considered that preservation is more relevant than magma generation for crustal net growth, with peaks in crystallization ages reflecting biases in preservation rather than magma production (Hawkesworth et al., 2009). Appropriately, the estimated preservation rates agree with the post-collisional batholiths playing a major role in crustal growth, since the preservation potential of new igneous rocks reaches a maximum in the post-collisional stage of the supercontinent cycle (Condie et al., 2011; Hawkesworth et al., 2009). This enhanced preservation potential is due to the rocks being shielded in the new orogens produced in each supercontinent cycle and mostly located towards its core. This results in an important contribution to the creation of long-term lived continental crust (Couzinié et al., 2016; Hawkesworth et al., 2010).

The two described factors support the role of post-collisional magmatism as a crustal growth mechanism. Both the generation

and preservation rates are explained by holding post-collisional magmas partially responsible for crustal growth. Additionally, natural evidence provided by outcropping rocks shows that this magmatism has been present throughout most of the history of the planet, associated with large scale orogenic process and supercontinent assembly. However, it has been particularly abundant in post-Archean times, producing a significant magmatic input during the most recent supercontinents formation. If this magma is mantle derived the stablished crustal growth paradigms must be revised, since the crustal growth associated with it may have been severely underestimated.

6. Conclusions

While the post-collisional mafic suite has recently been demonstrated to be a limited crustal growth mechanism, the more voluminous silicic suite has historically been dismissed in the crustal growth discussion due to bias imposed by the notion that it derives from a mostly recycled crustal source. However, the data presented in this paper points to the different conclusion that post-collisional granitic magmas indeed represent crustal growth.

If the post-collisional magmas come from a fully recycled crustal source, they should display crustal isotopic signatures. However, provided data shows that all the presented batholiths have a significant mantle component, coincident with a metasomatized mantle model line calculated using the mafic magma associated to these intrusions. Furthermore, experimental data provides a mechanism for the generation of the granitic suites and reproduction of the post-collisional geochemical signature (high MgO and K_2O, low CaO, and high LILE and LREE) by only using a mantle derived parental magma. That is, differentiation from a sanukitoid (post-collisional mafic magma) parental magma reproduces the post-collisional geochemical signature, with additional contamination with its own residue further enhancing the high-Mg signature and accounting for the heterogeneity of the series. Therefore, the crustal component is ultimately not necessary for the reproduction of the post-collisional granitic batholiths during batholith generation and emplacement, being the continental-like signature already present in the mantle source. This petrological argument points to the conclusion that post-collisional magmas represent the addition of juvenile material to the continental crust.

The generation of continental crust by post-collisional magmatism is also coherent with the observed generation and preservation rates within each supercontinent cycle. The existing models reveal the overlap between peaks in the continental crust production and orogenic to post-orogenic processes, correlating the post-collisional stage with the largest mantle derived magmatic input to the crust. Additionally, the preservation rates of magmas also reach maxima in the post-collisional stage, with the magmas shielded in the core of the orogens that amalgamated the supercontinents.

All presented arguments stablish a mechanism that can generate new continental crust in the most appropriate moment to allow its long-term preservation. Existing models must be revisited considering the given evidence, since post-Archean crustal growth may have been severely underestimated.

CRediT authorship contribution statement

Daniel Gómez-Frutos: Conceptualization, Data curation, Formal analysis, Investigation, Methodology, Validation, Visualization, Writing – original draft, Writing – review & editing. **Antonio Castro:** Conceptualization, Funding acquisition, Investigation, Methodology, Project administration, Supervision, Validation, Writing – review & editing. **Gabriel Gutiérrez-Alonso:** Conceptualization, Funding acquisition, Supervision, Writing – review & editing.

Declaration of competing interest

The authors declare that they have no known competing financial interests or personal relationships that could have appeared to influence the work reported in this paper.

Data availability

The compiled and experimental data is available in the online Supplementary Material.

Acknowledgements

This work was supported through the Spanish Research Agency (AEI) Grant N° PGC2018-096534-B-I00 (Proyecto IBERCRUST). We acknowledge the support received from the Instituto Andaluz de Ciencias de la Tierra (CSIC - UGR) and its staff for the installation of a high-pressure laboratory. We are particularly grateful to Taras Gerya and Mike Fowler for their positive and constructive feedback. We also want to thank Rosemary Hickey-Vargas for her handling of this manuscript.

Appendix A. Supplementary material

Supplementary material related to this article can be found online at https://doi.org/10.1016/j.epsl.2022.117978.

References

Annen, C., Blundy, J.D., Sparks, R.S.J., 2006. The genesis of intermediate and silicic magmas in deep crustal hot zones. J. Petrol. 47 (3), 505–539. https://doi.org/10.1093/petrology/egi084.

Aranovich, L.Y., Makhluf, A.R., Manning, C.E., Newton, R.C., 2014. Dehydration melting and the relationship between granites and granulites. Precambrian Res. 253, 26–37. https://doi.org/10.1016/j.precamres.2014.07.004.

Arndt, N.T., Goldstein, S.L., 1987. Use and abuse of crust-formation ages. Geology 15 (10), 893–895. https://doi.org/10.1130/0091-7613(1987)15<893:UAAOCA>2.0.CO;2.

Arndt, N.T., 2013. The formation and evolution of the continental crust. Geochem. Perspect. 2 (3), 405.

Barbarin, B., 1999. A review of the relationships between granitoid types, their origins and their geodynamic environments. Lithos 46 (3), 605–626. https://doi.org/10.1016/S0024-4937(98)00085-1.

Barth, M.G., McDonough, W.F., Rudnick, R.L., 2000. Tracking the budget of Nb and Ta in the continental crust. Chem. Geol. 165 (3–4), 197–213. https://doi.org/10.1016/S0009-2541(99)00173-4.

Belousova, E.A., Kostitsyn, Y.A., Griffin, W.L., Begg, G.C., O'Reilly, S.Y., Pearson, N.J., 2010. The growth of the continental crust: constraints from zircon Hf-isotope data. Lithos 119 (3–4), 457–466. https://doi.org/10.1016/j.lithos.2010.07.024.

Bonin, B., 2004. Do coeval mafic and felsic magmas in post-collisional to within-plate regimes necessarily imply two contrasting, mantle and crustal, sources? A review. Lithos 78 (1–2), 1–24. https://doi.org/10.1016/j.lithos.2004.04.042.

Castro, A., Moreno-Ventas, I., Fernández, C., Vujovich, G., Gallastegui, G., Heredia, N., Martino, R.D., Becchio, R., Corretgé, L.G., Díaz-Alvarado, J., Such, P., García-Arias, M., Liu, D.Y., 2011. Petrology and SHRIMP U–Pb zircon geochronology of Cordilleran granitoids of the Bariloche area, Argentina. J. South Am. Earth Sci. 32 (4), 508–530. https://doi.org/10.1016/j.jsames.2011.03.011.

Castro, A., Vogt, K., Gerya, T., 2013. Generation of new continental crust by sublithospheric silicic-magma relamination in arcs: a test of Taylor's andesite model. Gondwana Res. 23 (4), 1554–1566. https://doi.org/10.1016/j.gr.2012.07.004.

Castro, A., 2020. The dual origin of I-type granites: the contribution from experiments. Geol. Soc. (Lond.) Spec. Publ. 491 (1), 101–145. https://doi.org/10.1144/SP491-2018-110.

Castro, A., 2021. A non-basaltic experimental cotectic array for calc-alkaline batholiths. Lithos 382, 105929. https://doi.org/10.1016/j.lithos.2020.105929.

Cawood, P.A., Kroner, A., Pisarevsky, S., 2006. Precambrian plate tectonics: criteria and evidence. GSA Today 16 (7), 4. https://doi.org/10.1130/GSAT01607.1.

Cawood, P.A., Hawkesworth, C.J., Dhuime, B., 2013. The continental record and the generation of continental crust. GSA Bull. 125 (1–2), 14–32. https://doi.org/10.1130/B30722.1.

Chappell, B.W., Stephens, W.E., 1988. Origin of infracrustal (I-type) granite magmas. Earth Environ. Sci. Trans. R. Soc. Edinb. 79 (2–3), 71–86. https://doi.org/10.1017/S0263593300014139.

Chappell, B.W., White, A.J., 2001. Two contrasting granite types: 25 years later. Aust. J. Earth Sci. 48 (4), 489–499. https://doi.org/10.1046/j.1440-0952.2001.00882.x.
Collins, W.J., Huang, H.Q., Jiang, X., 2016. Water-fluxed crustal melting produces Cordilleran batholiths. Geology 44 (2), 143–146. https://doi.org/10.1130/G37398.1.
Condie, K.C., Aster, R.C., 2010. Episodic zircon age spectra of orogenic granitoids: the supercontinent connection and continental growth. Precambrian Res. 180 (3–4), 227–236. https://doi.org/10.1016/j.precamres.2010.03.008.
Condie, K.C., Bickford, M.E., Aster, R.C., Belousova, E., Scholl, D.W., 2011. Episodic zircon ages, Hf isotopic composition, and the preservation rate of continental crust. GSA Bull. 123 (5–6), 951–957. https://doi.org/10.1130/B30344.1.
Condie, K.C., 2014. Growth of continental crust: a balance between preservation and recycling. Mineral. Mag. 78 (3), 623–637. https://doi.org/10.1180/minmag.2014.078.3.11.
Couzinié, S., Laurent, O., Moyen, J.F., Zeh, A., Bouilhol, P., Villaros, A., 2016. Post-collisional magmatism: crustal growth not identified by zircon Hf–O isotopes. Earth Planet. Sci. Lett. 456, 182–195. https://doi.org/10.1016/j.epsl.2016.09.033.
Dewey, J.F., Windley, B.F., 1981. Growth and differentiation of the continental crust. Philos. Trans. R. Soc. Lond. Ser. A, Math. Phys. Sci. 301 (1461), 189–206. https://doi.org/10.1098/rsta.1981.0105.
Dhuime, B., Hawkesworth, C., Cawood, P., 2011. When continents formed. Science 331 (6014), 154–155. https://doi.org/10.1126/science.1201245.
Dhuime, B., Hawkesworth, C.J., Cawood, P.A., Storey, C.D., 2012. A change in the geodynamics of continental growth 3 billion years ago. Science 335 (6074), 1334–1336. https://doi.org/10.1126/science.1216066.
Dhuime, B., Hawkesworth, C.J., Delavault, H., Cawood, P.A., 2018. Rates of generation and destruction of the continental crust: implications for continental growth. Philos. Trans. R. Soc. A, Math. Phys. Eng. Sci. 376 (2132), 20170403. https://doi.org/10.1098/rsta.2017.0403.
Faccenda, M., Gerya, T.V., Chakraborty, S., 2008. Styles of post-subduction collisional orogeny: influence of convergence velocity, crustal rheology and radiogenic heat production. Lithos 103 (1–2), 257–287. https://doi.org/10.1016/j.lithos.2007.09.009.
Fowler, M.B., Henney, P.J., 1996. Mixed Caledonian appinite magmas: implications for lamprophyre fractionation and high Ba-Sr granite genesis. Contrib. Mineral. Petrol. 126 (1), 199–215. https://doi.org/10.1007/s004100050244.
Fowler, M.B., Henney, P.J., Darbyshire, D.P.F., Greenwood, P.B., 2001. Petrogenesis of high Ba–Sr granites: the Rogart pluton, Sutherland. J. Geol. Soc. 158 (3), 521–534. https://doi.org/10.1144/jgs.158.3.52.
Fowler, M.B., Kocks, H., Darbyshire, D.P.F., Greenwood, P.B., 2008. Petrogenesis of high Ba–Sr plutons from the northern highlands Terrane of the British Caledonian Province. Lithos 105 (1–2), 129–148. https://doi.org/10.1016/j.lithos.2008.03.003.
Fowler, M., Rollinson, H., 2012. Phanerozoic sanukitoids from Caledonian Scotland: implications for Archean subduction. Geology 40 (12), 1079–1082. https://doi.org/10.1130/G33371.1.
Gómez-Frutos, D., Castro, A., 2022. Sanukitoid crystallization relations at 1.0 and 0.3 GPa. Lithos 414, 106632. https://doi.org/10.1016/j.lithos.2022.106632.
Griffin, W.L., Pearson, N.J., Belousova, E., Jackson, S.E., van Achterbergh, E., O'Reilly, S.Y., Shee, S.R., 2000. The Hf isotope composition of cratonic mantle: LAM-MC-ICPMS analysis of zircon megacrysts in kimberlites. Geochim. Cosmochim. Acta 64, 133–147. https://doi.org/10.1016/S0016-7037(99)00343-9.
Hacker, B.R., Kelemen, P.B., Behn, M.D., 2011. Differentiation of the continental crust by relamination. Earth Planet. Sci. Lett. 307 (3–4), 501–516. https://doi.org/10.1016/j.epsl.2011.05.024.
Hawkesworth, C., Cawood, P., Kemp, T., Storey, C., Dhuime, B., 2009. A matter of preservation. Science 323 (5910), 49–50. https://doi.org/10.1126/science.1168549.
Hawkesworth, C.J., Dhuime, B., Pietranik, A.B., Cawood, P.A., Kemp, A.I., Storey, C.D., 2010. The generation and evolution of the continental crust. J. Geol. Soc. 167 (2), 229–248.
Hawkesworth, C., Cawood, P.A., Dhuime, B., 2019. Rates of generation and growth of the continental crust. Geosci. Front. 10 (1), 165–173. https://doi.org/10.1016/j.gsf.2018.02.004.
Herrmann, W., Berry, R.F., 2002. MINSQ–a least squares spreadsheet method for calculating mineral proportions from whole rock major element analyses. Geochem., Explor. Environ. Anal. 2 (4), 361–368. https://doi.org/10.1144/1467-787302-010.
Hildebrand, R.S., Whalen, J.B., 2017. The Tectonic Setting and Origin of Cretaceous Batholiths Within the North American Cordillera: the Case for Slab Failure Magmatism and Its Significance for Crustal Growth, vol. 532. Geological Society of America.
Jagoutz, O., Kelemen, P.B., 2015. Role of arc processes in the formation of continental crust. Annu. Rev. Earth Planet. Sci. 43, 363–404. https://doi.org/10.1146/annurev-earth-040809-152345.
Kemp, A.I.S., Hawkesworth, C.J., Paterson, B.A., Kinny, P.D., 2006. Episodic growth of the Gondwana supercontinent from hafnium and oxygen isotopes in zircon. Nature 439, 580–583. https://doi.org/10.1038/nature04505.
Meissner, R., Marshall, J., Plumb, R.A., 1986. The Continental Crust: a Geophysical Approach, vol. 34. Academic Press.
Moyen, J.F., Laurent, O., Chelle-Michou, C., Couzinié, S., Vanderhaeghe, O., Zeh, A., Villaros, A., Gardien, V., 2017. Collision vs. subduction-related magmatism: two contrasting ways of granite formation and implications for crustal growth. Lithos 277, 154–177. https://doi.org/10.1016/j.lithos.2016.09.018.
Nielsen, S.G., Marschall, H.R., 2017. Geochemical evidence for mélange melting in global arcs. Sci. Adv. 3 (4), e1602402. https://doi.org/10.1126/sciadv.1602402.
Orejana, D., Villaseca, C., Pérez-Soba, C., López-García, J.A., Billström, K., 2009. The Variscan gabbros from the Spanish Central System: a case for crustal recycling in the sub-continental lithospheric mantle? Lithos 110 (1–4), 262–276. https://doi.org/10.1016/j.lithos.2009.01.003.
Payne, J.L., McInerney, D.J., Barovich, K.M., Kirkland, C.L., Pearson, N.J., Hand, M., 2016. Strengths and limitations of zircon Lu-Hf and O isotopes in modelling crustal growth. Lithos 248, 175–192. https://doi.org/10.1016/j.lithos.2015.12.015.
Petford, N., Gallagher, K., 2001. Partial melting of mafic (amphibolitic) lower crust by periodic influx of basaltic magma. Earth Planet. Sci. Lett. 193 (3–4), 483–499. https://doi.org/10.1016/S0012-821X(01)00481-2.
Pitcher, W.S., 1987. Granites and yet more granites forty years on. Geol. Rundsch. 76 (1), 51–79. https://doi.org/10.1007/BF01820573.
Plank, T., Kelley, K.A., Zimmer, M.M., Hauri, E.H., Wallace, P.J., 2013. Why do mafic arc magmas contain ~4 wt% water on average? Earth Planet. Sci. Lett. 364, 168–179. https://doi.org/10.1016/j.epsl.2012.11.044.
Roberts, N.M., Spencer, C.J., 2015. The zircon archive of continent formation through time. Geol. Soc. (Lond.) Spec. Publ. 389 (1), 197–225. https://doi.org/10.1144/SP389.14.
Rudnick, R.L., 1995. Making continental crust. Nature 378 (6557), 571–578. https://doi.org/10.1038/378571a0.
Rudnick, R.L., Fountain, D.M., 1995. Nature and composition of the continental crust: a lower crustal perspective. Rev. Geophys. 33 (3), 267–309. https://doi.org/10.1029/95RG01302.
Rudnick, R.L., Gao, S., Holland, H.D., Turekian, K.K., 2003. Composition of the continental crust. The Crust 3, 1–64.
Shirey, S.B., Hanson, G.N., 1984. Mantle-derived Archaean monzodiorites and trachyandesites. Nature 310 (5974), 222–224. https://doi.org/10.1038/310222a0.
Smithies, R.H., Champion, D.C., 2000. The Archaean high-Mg diorite suite: links to tonalite–trondhjemite–granodiorite magmatism and implications for early Archaean crustal growth. J. Petrol. 41 (12), 1653–1671. https://doi.org/10.1093/petrology/41.12.1653.
Smithies, R.H., Lu, Y., Kirkland, C.L., Johnson, T.E., Mole, D.R., Champion, D.C., Martin, L., Jeon, H., Michael, T.D., Johnson, S.P., 2021. Oxygen isotopes trace the origins of Earth's earliest continental crust. Nature 592 (7852), 70–75. https://doi.org/10.1038/s41586-021-03337-1.
Spencer, C.J., Roberts, N.M.W., Santosh, M., 2017. Growth, destruction, and preservation of Earth's continental crust. Earth-Sci. Rev. 172, 87–106. https://doi.org/10.1016/j.earscirev.2017.07.013.
Stephens, W.E., 2001. Polycrystalline amphibole aggregates (clots) in granites as potential I-type restite: an ion microprobe study of rare-Earth distributions. Aust. J. Earth Sci. 48 (4), 591–601. https://doi.org/10.1046/j.1440-0952.2001.00880.x.
Stern, R.A., Hanson, G.N., Shirey, S.B., 1989. Petrogenesis of mantle-derived, LILE-enriched Archean monzodiorites and trachyandesites (sanukitoids) in southwestern Superior Province. Can. J. Earth Sci. 26 (9), 1688–1712. https://doi.org/10.1139/e89-145.
Ueda, K., Gerya, T.V., Burg, J.P., 2012. Delamination in collisional orogens: thermomechanical modeling. J. Geophys. Res., Solid Earth 117 (B8). https://doi.org/10.1029/2012JB009144.
Voice, P.J., Kowalewski, M., Eriksson, K.A., 2011. Quantifying the timing and rate of crustal evolution: global compilation of radiometrically dated detrital zircon grains. J. Geol. 119 (2), 109–126. https://doi.org/10.1086/658295.
Weinberg, R.F., Hasalová, P., 2015. Water-fluxed melting of the continental crust: a review. Lithos 212, 158–188. https://doi.org/10.1016/j.lithos.2014.08.021.
Wood, B.J., Turner, S.P., 2009. Origin of primitive high-Mg andesite: constraints from natural examples and experiments. Earth Planet. Sci. Lett. 283 (1–4), 59–66. https://doi.org/10.1016/j.epsl.2009.03.032.